Journal of Applied Polymer Science

Biomineralized Hyaluronic Acid/Poly(vinylphosphonic acid) Hydrogel for Bone Tissue Regeneration

So Yeon Kim,[1] Jeong-Sook Park[2]

[1]Department of Chemical Engineering Education, College of Education, Chungnam National University, Daejeon 305-764, South Korea

[2]Department of Physical Pharmacy, College of Pharmacy, Chungnam National University, Daejeon 305-764, South Korea

Correspondence to: S. Y. Kim (E-mail: kimsy@cnu.ac.kr)

ABSTRACT: Novel biomineralized hydrogels composed of hyaluronic acid (HA) and vinyl phosphonic acid (VPAc) were designed with the aim of developing a biomimetic hydrogel system to improve bone regeneration by local delivery of a protein drug including bone morphogenetic proteins. We synthesized crosslinked hydrogels composed of methacrylated HA and poly(VPAc) [P(VPAc)], which serves as a binding site for calcium ions during the mineralization process. The HA/P(VPAc) hydrogels were biomineralized by a urea-mediation method to create functional polymer hydrogels that can deliver the protein drug and mimic the bone extracellular matrix. The water content of the hydrogels was influenced by the HA/P(VPAc) composition, crosslinking density, biomineralization, and ionic strength of the swelling media. All HA/P(VPAc) hydrogels maintained more than 84% water content. Enzymatic degradation of HA/P(VPAc) hydrogels was dependent on the concentration of hyaluronidase and the crosslinking density of the polymer network within the hydrogel. In addition, the release behavior of bovine serum albumin from the HA/PVPAc hydrogels was mainly influenced by the drug loading content, water content, and biomineralization of the hydrogels. In a cytotoxicity study, the HA/P(VPAc) and biomineralized HA/P(VPAc) hydrogels did not significantly affect cell viability. These results suggest that biomineralized HA/P(VPAc) hydrogels can be tailored to create a biomimetic hydrogel system that promotes bone tissue repair and regeneration by local delivery of protein drugs. © 2014 Wiley Periodicals, Inc. J. Appl. Polym. Sci. **2014**, *131*, 41194.

KEYWORDS: biomaterials; drug delivery systems; gels

Received 1 April 2014; accepted 18 June 2014

DOI: 10.1002/app.41194

INTRODUCTION

A bone replacement matrix has been developed for osteogenic promotion and replacement of injured bone tissues.[1–5] Recent advances in biotechnology have resulted in a great variety of pharmaceutically active peptides and proteins[6,7]; however, these agents are often cleared rapidly from the circulation and therefore need to be administered frequently to maintain therapeutic levels in the blood.[6–10] Because one of the major issues limiting the therapeutic applicability of protein-based drugs is the lack of suitable dosage forms, there is a great demand for novel methods of delivering these drugs and new drug release strategies.[6–10]

Hydrogels are considered interesting carriers/vessels for peptide and protein delivery because of their good tissue compatibility and the possibilities for manipulating their permeability for drug molecules.[11–15] Furthermore, hydrogels have proven useful in the investigation of many aspects of biomineralization in different *in vitro* environments.[16–18]

Natural bone is a composite of collagen, a protein-based hydrogel template, and inorganic dahilite (carbonated apatite) crystals.[4] It was reported that acidic extracellular matrix proteins attached to the collagen scaffolds play important inhibitory roles and function as a template during the mineralization process.[16–18] The acidic groups serve as binding sites for calcium ions and align them in an orientation that matches the apatite crystal lattice.[16,17]

Mineralized polymeric matrices have emerged as promising tools to uncover the complex roles of the cellular microenvironment in regulating the diverse phenotypic activities of stem and progenitor cells related to the development, repair, regeneration, and remodeling of bone tissue.[19,20] Most of the studies focused on the apatite formation on gels, scaffolds, fibers, or grafted films.[16–18,21–23] Several pioneering works have tried to understand and shown that the role of chemical motifs should be mediated by other matrix variables, such as pore size and the density of hydrophobic motifs, specifically for the mineralization of a three dimensional matrix.[24–26] However, biomineralized hydrogel system for local delivery of a protein drug has not yet been systematically examined.

The main objective of this study was to prepare a biomimetic hydrogel system to improve bone regeneration by local delivery

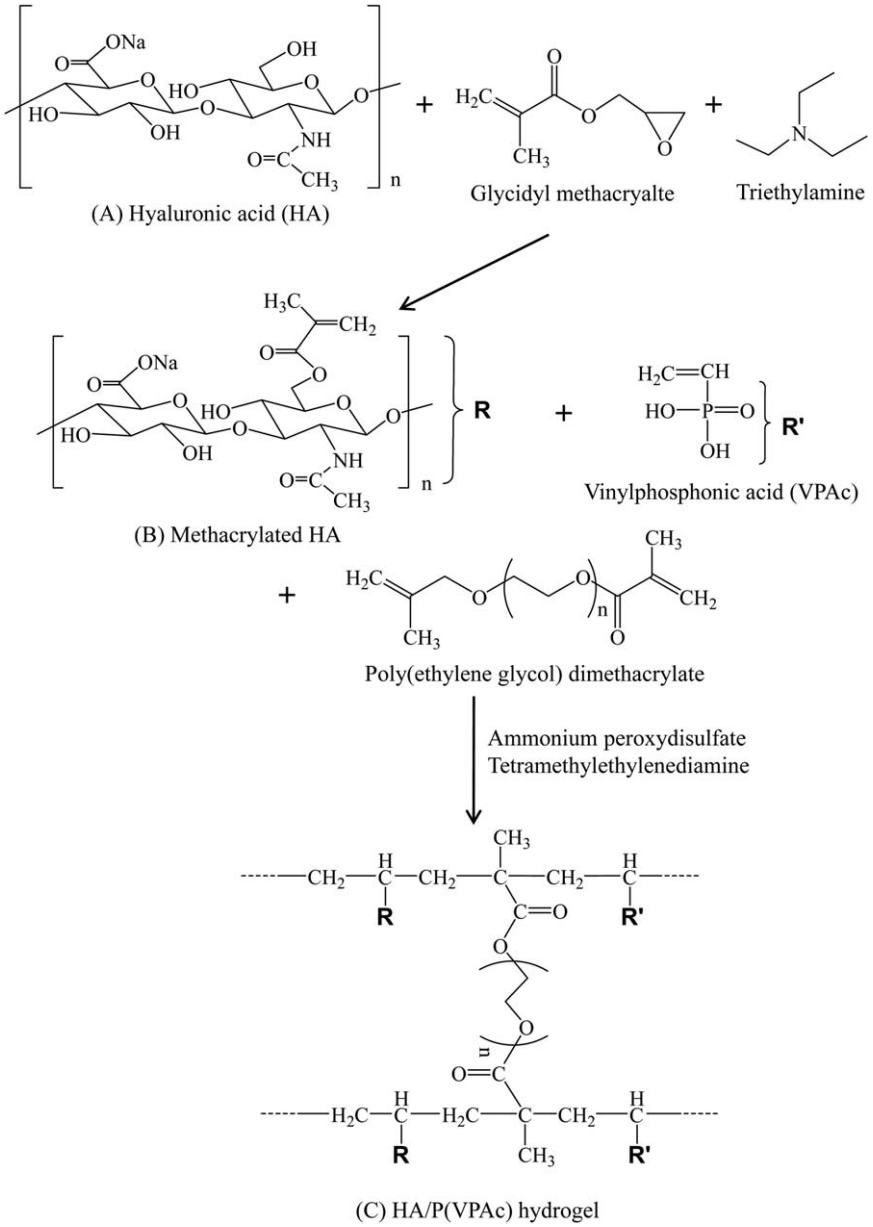

Figure 1. Synthetic scheme for HA/P(VPAc) hydrogels; (A) HA, (B) methacrylated HA, and (C) HA/P(VPAc) hydrogel.

of a protein drug including bone morphogenetic proteins. An optimized delivery system might improve the osteopotency of the device while reducing the amount of introduced therapeutic proteins and peptides, which offers the double advantage of being safer as well as less expensive.

In this study, we focused on biomineralized hyaluronic acid (HA)-based hydrogels. HA is an important component of synovial fluid and extracellular matrices, therefore it could be an attractive building block in new biocompatible and biodegradable polymers for the promotion of wound healing and tissue regeneration.[27–29]

In the present study, a HA derivative with crosslinkable methacrylate groups was used to prepare crosslinked hydrogels composed of HA and vinyl phosphonic acid (VPAc), which serves as a binding site for calcium ions during the mineralization process. To evaluate the feasibility of biomineralized HA/P(VPAc) hydrogels to deliver a protein drug and mimic the bone extracellular matrix, we characterized their morphology, water content, and enzymatic degradation kinetics. The *in vitro* release behavior of a model protein drug from the HA/P(VPAc) hydrogels and biocompatibility of the hydrogels were also evaluated.

MATERIALS AND METHODS

Materials

HA (from *Streptococcus equi sp.*, $M_w = 1.6 \times 10^6$ Da), vinylphosphonic acid (VPAc), poly(ethylene glycol) dimethacrylate (PEGDM), triethylamine (TEA), glycidyl methacrylate (GM), ammonium peroxydisulfate, hydroxyapatite, and *N,N,N′,N′*-tetramethylethylenediamine (TEMED) were purchased from Sigma

Table I. Composition of HA/P(VPAc) and Biomineralized HA/P(VPAc) Hydrogels

No.	Hydrogel sample[a]	HA/VPAc monomer weight ratio in feed[b]	Crosslinker (PEGDM; mmol)	Biomineralization
1	HA/P(VPAc)10/0-2	10 : 0	1.11	-
2	HA/P(VPAc)9/1-2	9 : 1	1.11	-
3	HA/P(VPAc)8/2-2	8 : 2	1.11	-
4	B-HA/P(VPAc)10/0-2	10 : 0	1.11	✓
5	B-HA/P(VPAc)9/1-2	9 : 1	1.11	✓
6	B-HA/P(VPAc)8/2-2	8 : 2	1.11	✓
7	HA/P(VPAc)10/0-1	10 : 0	0.74	-
8	HA/P(VPAc)10/0-3	10 : 0	2.22	-
9	HA/P(VPAc)10/0-4	10 : 0	3.71	-
10	HA/P(VPAc)9/1-1	9 : 1	0.74	-
11	HA/P(VPAc)9/1-3	9 : 1	2.22	-
12	HA/P(VPAc)9/1-4	9 : 1	3.71	-
13	HA/P(VPAc)8/2-1	8 : 2	0.74	-
14	HA/P(VPAc)8/2-3	8 : 2	2.22	-
15	HA/P(VPAc)8/2-4	8 : 2	3.71	-

[a] All hydrogels were synthesized in distilled water as a reaction solvent.
[b] The total amount of HA and VPAc in feed was 3 w/v% of the reaction media.

(St. Louis, MO). Urea and hydrogen chloride were obtained from Aldrich (Milwaukee, WI) and Chemical (Tokyo, Japan), respectively. Dulbecco's phosphate-buffered saline (PBS), Dulbecco's Modified Eagle Medium (DMEM, high glucose, with L-glutamine, with pyridoxine hydrochloride, without sodium pyruvate), and heat-inactivated fetal bovine serum (FBS) were purchased from GIBCO BRL (Grand Island, NY). Bovine serum albumin (BSA) was purchased from Sigma. Distilled and deionized water was prepared using a Milli-Q Plus System (Millipore, Bedford, MA). All other chemicals used were reagent grade and were used as purchased without further purification.

Methods

Synthesis of Methacrylated HA. One gram of HA [Figure 1(A)] was dissolved completely in 100 mL distilled water and then TEA and GM were added separately (2.2–5.0 mL). The reaction mixture was thoroughly mixed for 1 h at 60°C and stirred overnight at room temperature. After reaction, the solution was precipitated in a 20-fold volumetric excess of acetone and dissolved in distilled water twice to remove excess reactants. The methacrylated HA solution was lyophilized and stored desiccated at 4°C. The chemical structure of methacrylated HA [Figure 1(B)] was analyzed by 400 MHz ^{1}H NMR (JNM-AL400, JEOL, Tokyo, Japan) and Fourier transform infrared spectroscopy (FTIR) (FT/IR-460 PLUS spectrometer, JASCO, Tokyo, Japan).

Preparation of HA/P(VPAc) Hydrogels. Crosslinked HA/P(VPAc) hydrogels were prepared at room temperature by simultaneous free radical polymerization and crosslinking as shown in Figure 1(C). The hydrogels were prepared by varying the weight ratio of methacrylated HA/VPAc and the amount of crosslinker in the feed. The feed weight ratio of methacrylated HA/VPAc changed from 10/0 to 8/2. The polymerization formulations of hydrogels are described in Table I.

Dry nitrogen gas was bubbled through 0.45 g of a mixture of methacrylated HA and VPAc and PEGDM (0.74–3.71 mmol) in distilled water for 15 min to remove dissolved oxygen. After the nitrogen gas purge, ammonium peroxysulfate (0.01 g) and TEMED (100 μL) were added as the initiator and accelerator, respectively. The mixture was stirred vigorously for 30 s and allowed to polymerize at room temperature for 24 h under regular fluorescent light in a glass vial. After polymerization, the HA/P(VPAc) hydrogel was washed three times for 3–5 min each in excess ultrapure water to remove compounds that had not reacted.

Biomineralization of HA/P(VPAc) Hydrogels. To improve the interaction between hydrogel and osteoblasts, biomineralization of the HA/P(VPAc) hydrogel was performed by a urea-mediated method.[16] Hydroxyapatite (2.92 mmol) was suspended in 100 mL deionized water with stirring, and 2*M* HCl was added sequentially until the hydroxyapatite suspension was completely dissolved at a final pH of 2.5–3. Urea (0.2 mol) was then dissolved in the solution to reach a concentration of 2*M*. Each of the HA/P(VPAc) hydrogel samples (1.5 cm × 1.5 cm × 2 mm) was immersed in 50 mL of the acidic HA-urea stock solution. The mineralization solution was slowly heated to 90–95°C within 2 h with an average heating rate of 0.6°C/min without agitation and maintained at that temperature overnight. The final pH was ~8.0. Mineralized HA/P(VPAc) hydrogel samples were repeatedly washed in ultrapure water to remove loosely attached minerals and soluble ions.

Characterization of HA/P(VPAc) and Biomineralized HA/P(VPAc) Hydrogels. The chemical structure of the HA/P(VPAc) and biomineralized HA/P(VPAc) hydrogels was confirmed by

FTIR measurements. FTIR spectra were recorded on a FT/IR-460 PLUS spectrometer (JASCO) ranging between 4000 and 650 cm^{-1}, with a resolution of 2 cm^{-1} and 64 scans.

The HA/P(VPAc) and biomineralized HA/P(VPAc) hydrogel samples were freeze-dried overnight, weighed upon removal from the freeze-dryer, and immersed in excess ultrapure water and PBS for 24 h at 37°C. The water content was calculated on the basis of the weight difference of the hydrogel samples before and after swelling:

$$\text{Water content } (\%) = (W_s - W_d)/W_s \times 100, \quad (1)$$

where W_s is the weight of the swollen gel and W_d is the weight of the dry gel.

The surface and cross-section morphology of the HA/P(VPAc) and biomineralized HA/P(VPAc) hydrogels was examined by field emission scanning electron microscopy (FE-SEM) (JSM-7000F, JEOL, Tokyo, Japan) at 15 kV.

Enzymatic Degradation of HA/P(VPAc) Hydrogels. Enzymatic degradation of HA/P(VPAc) hydrogels was investigated by monitoring the mass loss of the hydrogel samples as a function of time of exposure to an enzyme solution.[30,31] The relationship between degradation behavior of the HA/P(VPAc) hydrogels and the concentration of hyaluronidase solution and the cross-linking density of hydrogel was investigated over 12 days. Each HA/P(VPAc) hydrogel sample (dimensions = 2.0 × 5.0 × 5.0 mm^3) was placed in PBS (pH = 7.4) in a shaking water bath at 37°C for 24 h and the initial weight of the swollen samples was measured. The hydrogels were then placed in PBS containing hyaluronidase, 0.2 mg/mL sodium azide and 1 m*M* $CaCl_2$, and shaken gently at 37°C. The mass loss of the hydrogel samples was tracked over time based on the initial swollen weight. Three specimens were tested for each sample. The remaining weight (%) of HA/P(VPAc) hydrogels was calculated using the following equation:

$$\text{Remaining weight } (\%) = (W_t/W_0) \times 100, \quad (2)$$

where W_0 is the initial weight of the hydrogel and W_t is the swollen weight of the hydrogel at each time point.

***In Vitro* Drug Release Behavior of HA/P(VPAc) and Biomineralized HA/P(VPAc) Hydrogels.** BSA (molecular weight = 65,000 Da, Fraction V, Sigma) was used as a model protein drug in the *in vitro* drug release test. BSA solution (50.0 mg/ mL) was prepared using deionized water. Previously dried HA/P(VPAc) and biomineralized HA/P(VPAc) hydrogel samples were soaked in 20 mL BSA solution for 1 day at 25°C and allowed to swell to an equilibrium state. The fully swollen hydrogels were blotted with filter paper to eliminate surface water and dried until they achieved a constant weight. The amount of drug loaded into the HA/P(VPAc) hydrogel was determined by the following equation:

$$\text{DLC}(\%) = \frac{\text{mass of BSA}}{\text{mass of BSA-loaded HA/P(VPAc) hydrogel}} \times 100 = \frac{\text{BSA}}{\text{BSA} + \text{hydrogel}} \times 100$$

Dried BSA-loaded HA/P(VPAc) hydrogel was placed in a 25-mL sealed vial containing PBS (0.1*M*, pH = 7.4) and incubated in a water bath (at 37 ± 0.5°C) with gentle shaking at 50 rpm. At predetermined time intervals, 3-mL aliquots of aqueous solution were withdrawn from the release medium and replaced with an equivalent volume of fresh buffer solution. The amount of BSA released was analyzed by UV-visible spectrophotometry (Shimadzu Model UV 2101PC, Kyoto, Japan) at 280 nm. The cumulative amount of released BSA was determined using the standard calibration curve. All release experiments were carried out in triplicate.

Biocompatibility Study. The *in vitro* cytotoxicity of the HA/P(VPAc) and biomineralized HA/P(VPAc) hydrogels was evaluated using an indirect extraction method.[32,33] Extracts were obtained by immersing fragments of each of the hydrogels (0.2 g/mL) in culture medium at 37°C. After incubation for 2 days, extracts of the hydrogel samples were collected and diluted to 25, 50, 75, and 100% with culture media. Human hepatoma HepG2 cells were obtained from the Korea Cell Line Bank and maintained in a culture medium composed of DMEM, 10% FBS, and 100 U/ mL penicillin-streptomycin. HepG2 cells were seeded in 96-well plates at a density of 2.0×10^4 cells/well and incubated at 37°C in a humidified 5% CO_2 atmosphere for 48 h. After the cells had attached to the wells, the initial culture medium was replaced with medium containing hydrogel extract and the cells were incubated for 48 h at 37°C. At the end of the incubation period, the extract medium was discarded and cell viability was determined using the MTT assay ($n = 4$). In brief, 50 μL of 3-(4,5-dimethylthiazol-2-yl)-2,5-diphenyl tetrazolium bromide (MTT) solution (12 m*M*) was added to each well. After 4-h incubation at 37°C, the MTT solution was removed and the insoluble formazan crystals that formed were dissolved in 150 μL dimethylsulfoxide. Absorbance of the formazan product was measured at 540 nm using a microplate reader (Tecan Trading, Mannedorf, Switzerland). The untreated cells served as a positive control and were taken as 100% viable.

RESULTS AND DISCUSSION

Synthesis of HA Derivatives

Methacrylation of HA was performed to synthesize HA derivatives with polymerizable residues [Figure 1 (B)]. Figure 2 shows the ^1H NMR spectra of native HA that served as a control [Figure 2(A)] and methacrylated HA [Figure 2(B,C)]. ^1H NMR spectrum confirmed the substitution of methacrylate groups on the HA backbone, showing not only peaks at ~1.9 ppm (peak b) and 3.0–4.4 ppm (peak a) corresponding to the methyl protons and the protons on the ring of original HA, respectively, but also two distinctive peaks at 5.6 and 6.0 ppm (peak f) that were attributed to the two protons of the double bond of the methacrylate group and a peak at ~1.8 ppm (peak e) ascribed to the methyl group adjacent to the double bond, which were not present in the

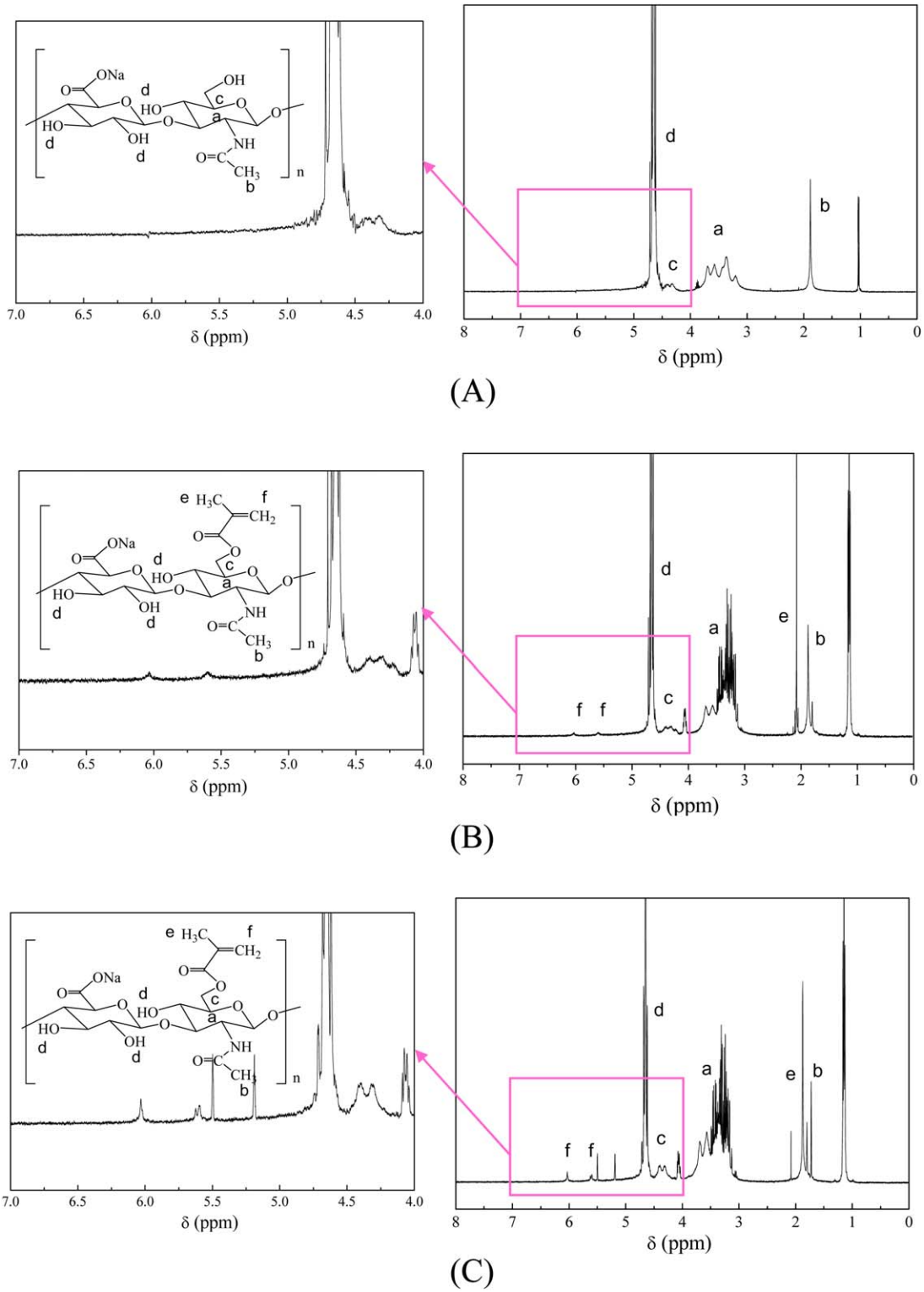

Figure 2. ^{1}H NMR spectra of (A) HA, (B) methacrylated HA prepared using 2.2 mL TEA and 2.2 mL GM, and (C) methacrylated HA prepared using 3.5 mL TEA and 3.5 mL GM. [Color figure can be viewed in the online issue, which is available at wileyonlinelibrary.com.]

original HA. In addition, the two distinctive peaks at 5.6 and 6.0 ppm (peak f) and thepeak at ~1.8 ppm (peak e) gradually increased with an increase in the feed ratio of TEA and GM during the methacrylation reaction, as shown in Figure 2(B,C). This indicates that methacrylated HA derivatives can be synthesized with controllable methacrylation percentages.

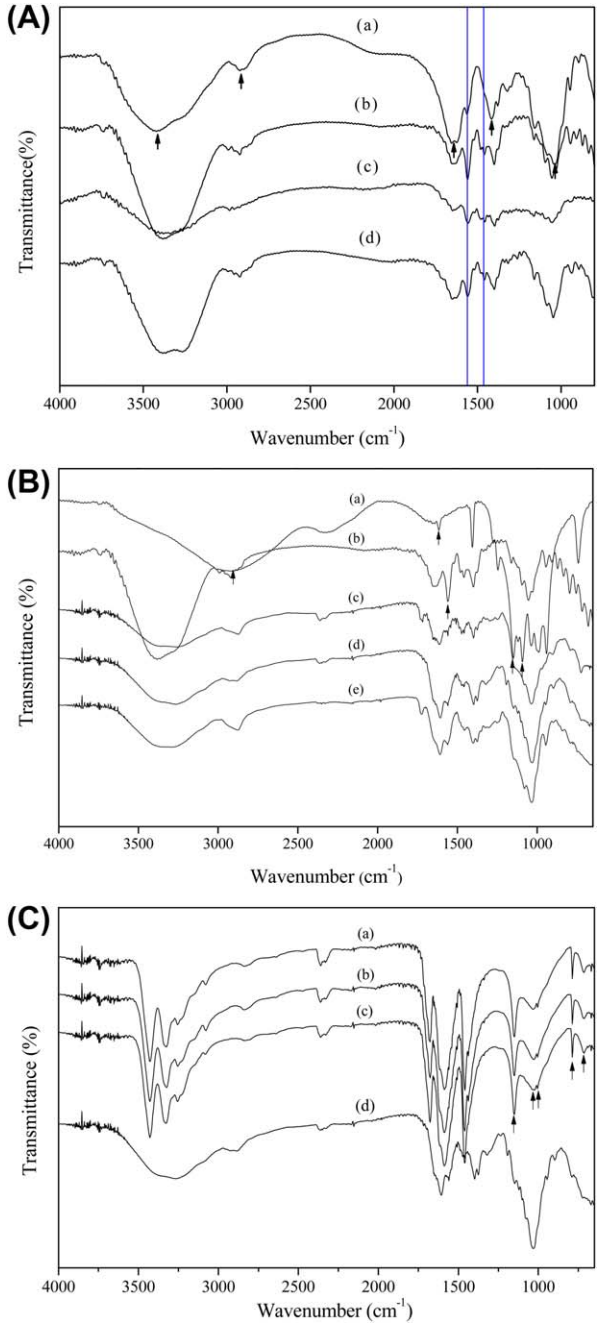

Figure 3. FTIR spectra of (A) methacrylated HA derivatives; (a) native HA, (b) methacrylated HA prepared using 2.2 mL TEA and 2.2 mL GM, (c) methacrylated HA prepared using 3.5 mL TEA and 3.5 mL GM, and (d) methacrylated HA prepared using 5.0 mL TEA and 5.0 mL GM; (B) HA/P(VPAc) hydrogels: (a) VPAc, (b) methacrylated HA, (c) HA/P(VPAc)8/2-2, (d) HA/P(VPAc)9/1-2, and (e) P(VPAc)10/0-2; (C) biomineralized HA/P(VPAc) hydrogels; (a) B-HA/P(VPAc)8/2-2, (b) B-HA/P(VPAc)9/1-2, (c) B-HA/P(VPAc)10/0-2, and (d) HA/P(VPAc)9/1-2. [Color figure can be viewed in the online issue, which is available at wileyonlinelibrary.com.]

Figure 3(A) shows the FTIR spectra of HA and methacrylated HA. For HA [Figure 3(A-a)], a characteristic peak was observed in the region of 3419 cm^{-1} due to hydrogen bonded O—H stretching and N—H stretching vibration of the N-acetyl side chain. The peaks at 1637 and 1415 cm^{-1} were assigned to the amide I group of C═O carboxyl and aromatic amine CN stretching, respectively. The peak at 2911 cm^{-1} was caused by the methyl C—H stretch corresponding to glucuronic acid. A peak at 1036 cm^{-1} for the primary alcohol C—O stretch was also observed. Compared with the original HA, methacrylated HA showed a sharp peak at ~1556 cm^{-1} (C═C) and a new peak at ~1459 cm^{-1} (CH_2═), representing the double bond of the methacrylate group [Figure 3(A-b–d)]. These results confirmed that HA was derivatized with methacrylated groups.

Characterization of HA/P(VPAc) and Biomineralized Hydrogels

HA/P(VPAc) hydrogels were prepared by varying the feed ratio of HA and VPAc as shown in Table I. FTIR spectroscopy measurements were carried out to confirm the synthesis of HA/P(VPAc) hydrogels. Figure 3(B) illustrates FTIR spectra of (a) VPAc, (b) methacrylated HA, (c) HA/P(VPAc)8/2-2, (d) HA/P(VPAc)9/1-2, and (e) HA/P(VPAc)-10/0-2 hydrogels.

As shown in Figure 3(B-a), the FTIR spectrum of VPAc exhibited a wide band at ~2910 cm^{-1} and peaks at 1615 and 1146 cm^{-1} corresponding to P═O stretching. The spectrum also contained absorption bands of the asymmetric stretching vibration of the P—O—H group at 1096 cm^{-1}. The methacrylated HA showed a sharp characteristic peak at ~1556 cm^{-1} (C═C) that can be attributed to the double bond of the methacrylate group [Figure 3(B-b)]. However, this peak was significantly reduced in the FTIR spectra of HA/P(VPAc) hydrogels [Figure 3(B-c)] HA/P(VPAc)8/2-2, (d) HA/P(VPAc)9/1-2, and (e) P(VPAc)10/0-2). In addition, the FTIR spectra of HA/P(VPAc) hydrogels included characteristic absorptions of both HA and VPAc, clearly indicating that HA/P(VPAc) hydrogels were successfully prepared by simultaneous free radical polymerization and crosslinking.

HA/P(VPAc) hydrogels were biomineralized by a urea-mediated method to create functional polymer hydrogels that can deliver protein drug and mimic the bone extracellular matrix. After biomineralization, the physical appearance of the HA/P(VPAc) hydrogels turned from transparent to white.

The morphologies of HA/P(VPAc) hydrogels before and after biomineralization were observed by FE-SEM measurement. Figure 4 shows the surface and cross-sectional morphologies of HA/P(VPAc) and biomineralized HA/P(VPAc) hydrogels. As shown in Figure 4(B), after the mineralization procedure a crystalline formation was observed within and on the surface of biomineralized HA/P(VPAc) hydrogels (B-HA/P(VPAc)9/1-2).

These biomineralized HA/P(VPAc) hydrogels were analyzed by FTIR spectroscopy. The FTIR spectra of the untreated HA/P(VPAc) hydrogels and the biomineralized HA/P(VPAc) hydrogels are compared in Figure 3(C). The presence of phosphate groups in both hydroxyapatite and the HA/P(VPAc) copolymer complicates characterization of the apatite growth obtained in the hydrogel samples because its bands overlap with the phosphate groups of the copolymer. After biomineralization, a strong band appeared at 1150 cm^{-1}. This has been attributed to the presence of phosphate salt, indicating that the interaction involves bonding of Ca ions with the P—O^- and P—O_4^{3-} ions of

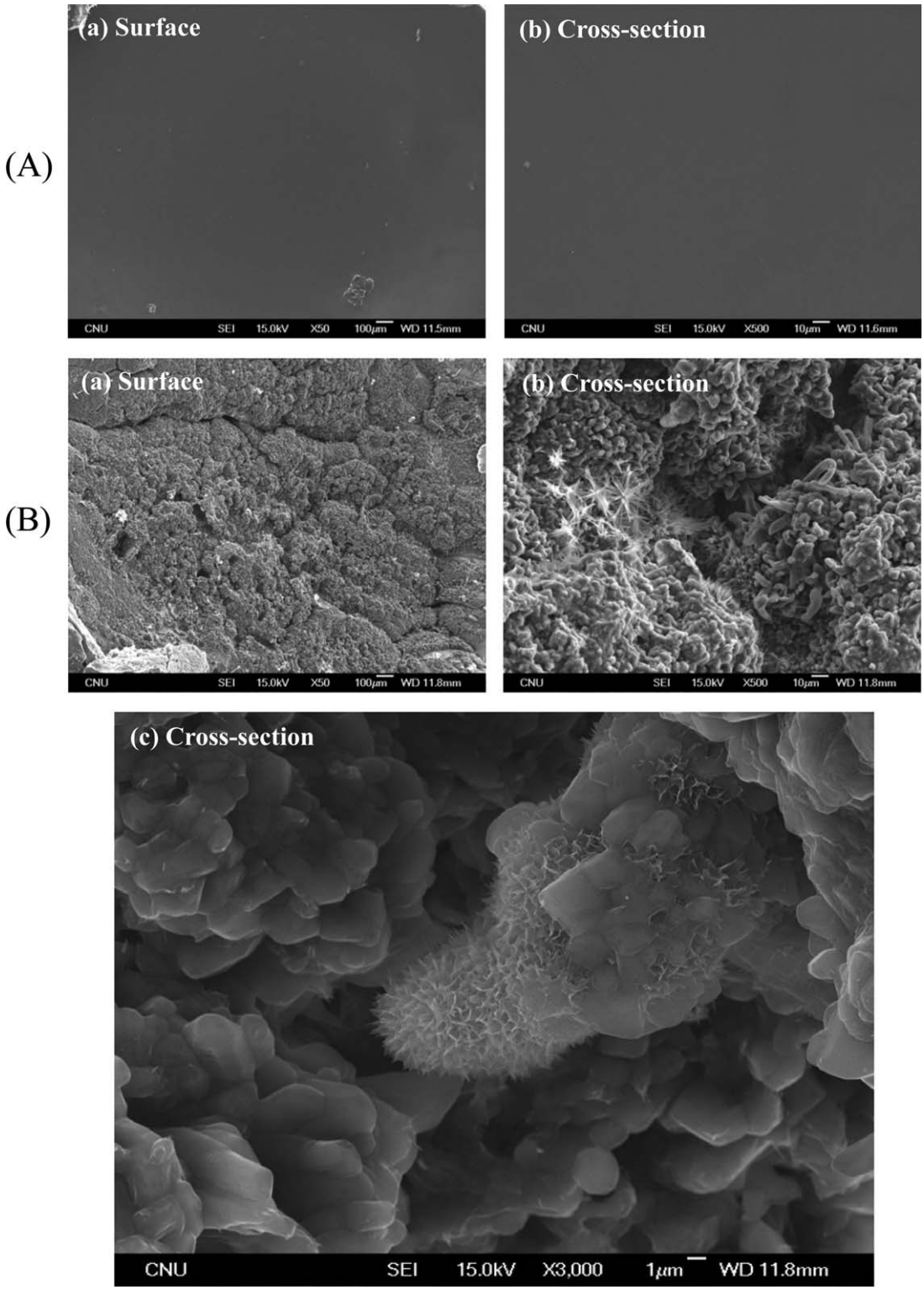

Figure 4. Surface and cross-sectional morphologies of HA/P(VPAc) and biomineralized HA/P(VPAc) hydrogels; (A) HA/P(VPAc)9/1-2 and (B) B-HA/P(VPAc)9/1-2.

the copolymer [Figure 3(C); (a) B-HA/P(VPAc)8/2-2, (b) B-HA/P(VPAc)9/1-2, and (c) B-HA/P(VPAc)10/0-2].

In addition, a band at 1005 cm^{-1} (assigned to the symmetric vibration of P—O), a band at 1024 cm^{-1} (assigned to the asymmetric vibration of P—O), and a band at 1150 cm^{-1} (assigned to the phosphonyl group P═O) were observed. The FTIR spectrum also shows characteristic peaks at 786 and 716 cm^{-1} that were derived from the hydroxyapatite. These results demonstrate the presence of hydroxyapatite in the HA/P(VPAc) hydrogel.

Table II. Water Content and DLC of HA/P(VPAc) and Biomineralized HA/P(VPAc) Hydrogels

No.	Hydrogel sample	Water[a]	PBS[a]	DLC (%)[b]
1	HA/P(VPAc)10/0-2	98.02 ± 0.12	96.51 ± 0.06	38.21 ± 1.78
2	HA/P(VPAc)9/1-2	97.82 ± 0.11	95.43 ± 0.60	35.74 ± 0.57
3	HA/P(VPAc)8/2-2	96.43 ± 0.02	94.48 ± 0.11	30.77 ± 1.76
4	B-HA/P(VPAc)10/0-2[c]	92.36 ± 0.39	87.73 ± 0.04	17.46 ± 0.41
5	B-HA/P(VPAc)9/1-2[c]	91.41 ± 0.08	86.07 ± 0.64	16.32 ± 2.87
6	B-HA/P(VPAc)8/2-2[c]	90.88 ± 0.54	84.46 ± 0.08	16.08 ± 1.56
7	HA/P(VPAc)10/0-1	98.53 ± 0.02	96.68 ± 0.13	-
8	HA/P(VPAc)10/0-3	97.18 ± 0.08	94.01 ± 0.04	-
9	HA/P(VPAc)10/0-4	95.90 ± 0.09	93.61 ± 0.06	-
10	HA/P(VPAc)9/1-1	97.95 ± 0.06	95.47 ± 0.13	-
11	HA/P(VPAc)9/1-3	97.39 ± 0.12	94.62 ± 0.55	-
12	HA/P(VPAc)9/1-4	94.63 ± 0.11	92.60 ± 0.06	-
13	HA/P(VPAc)8/2-1	97.13 ± 0.05	94.70 ± 0.36	-
14	HA/P(VPAc)8/2-3	95.97 ± 0.05	93.78 ± 0.06	-
15	HA/P(VPAc)8/2-4	94.37 ± 0.14	93.25 ± 0.85	-

[a] Water content of hydrogel = $(W_s - W_d)/W_s \times 100$, where W_s is weight of swollen gel and W_d is weight of dry gel. Each water content value represents the average of four samples.
[b] DLC = (mass of BSA/mass of BSA – loaded hydrogel) × 100 = [BSA/(BSA + polymer)] × 100.
[c] Biomineralized HA/P(VPAc) hydrogel samples.

Water Content of HA/P(VPAc) and Biomineralized HA/P(VPAc) Hydrogels

Table II shows the water content of the HA/P(VPAc) and biomineralized HA/P(VPAc) hydrogels in deionized water and PBS, respectively. All of the HA/P(VPAc) hydrogel samples exhibited a relatively high water content of >90% regardless of their composition. The water content gradually increased as the amount of HA ($pK_a = 3.0$) in the hydrogel increased. HA contains an ionizable group, $-COO^-$. The presence of ionized $-COO^-$ groups within the HA/P(VPAc) hydrogel causes repulsion between them, resulting in an increase in free volume in the polymeric matrix and thus an increase in swelling of the hydrogel. However, as the P(VPAc) content increased, the water content of the HA/P(VPAc) hydrogels gradually decreased. It can be proposed that the hydrophilic monomer VPAc did not significantly increase the water content of the hydrogel because the phosphonic acid groups did not fully ionize in the swelling medium (deionized water, pH = 5.8). Phosphonic acid groups in HA/P(VPAc) hydrogels dissociate to monobasic and dibasic species at pH values of ~3.1 (pK_1) and 9.0 (pK_2), respectively.[34]

The water content of biomineralized HA/P(VPAc) hydrogels was lower than that of untreated HA/P(VPAc) hydrogels irrespective of the HA and P(VPAc) composition (Table II). This suggests that the nucleation and growth of calcium phosphate in the hydrogels during biomineralization inhibits interaction between ionic groups in hydrogels and water molecules, leading to a reduction in water content.

In addition, the water content of the hydrogels was lower in PBS than in deionized water (Table II). The effect of the media on swelling behavior can be attributed to shielding of the $-COO^-$, $-PO_3H^-$, and $-PO_3^{2-}$ repulsion, which prevents collapse of the gel, by interactions between $-COO^-$, $-PO_3H^-$, and $-PO_3^{2-}$ groups in HA/P(VPAc) and ions present in the PBS.[35]

The effect of crosslinking density on the water content of HA/P(VPAc) hydrogels was also investigated (Table II). As the crosslinking density within the hydrogel increased (feed amount of PEGDM = 0.74–3.71 mmol) the water content gradually decreased, as shown in Table II and Figure 5. As the crosslinker concentration is increased, it increases the ability of polymer chain to get crosslinked.[36] In addition, HA/P(VPAc) hydrogels prepared using the same feed ratio of crosslinker exhibited a lower water content in PBS than in deionized water [Figure 5(B)].

Enzymatic Degradation Behavior of HA/P(VPAc) Hydrogels

The enzymatic degradation of HA/P(VPAc) hydrogels was determined by monitoring mass loss of the hydrogel samples as a function of time of exposure to a hyaluronidase solution (Figure 6). The *in vitro* degradation kinetics of the HA/P(PVAc) hydrogels with respect to the concentration of hyaluronidase solution (0–1000 U/ mL) and the crosslinking density within the hydrogel structure (feed amount of PEGDM = 0.74–3.71 mmol) were investigated. HA/P(VPAc)8/2-2 hydrogels showed significant weight loss in a hyaluronidase concentration-dependent manner [Figure 6(A)].

HA/P(VPAc)8/2-2 hydrogels in control solution without enzyme did not show any decrease in weight as a function of time whereas HA/P(VPAc)8/2-2 hydrogels in 30 U/mL hyaluronidase solution showed 46.5% degradation after 12 days of exposure and hydrogels in 1000 U/mL hyaluronidase solution were completely degraded within 138 h [Figure 6(A)].

The degradation of hydrogel in solution is generally associated with several network parameters such as the number of crosslinks per backbone chain, the number of vinyl groups on the crosslinking molecule, molecular weight of the backbone, and the proportion of degradable groups in the main and side chain. The degradation behavior of HA/P(VPAc) hydrogels

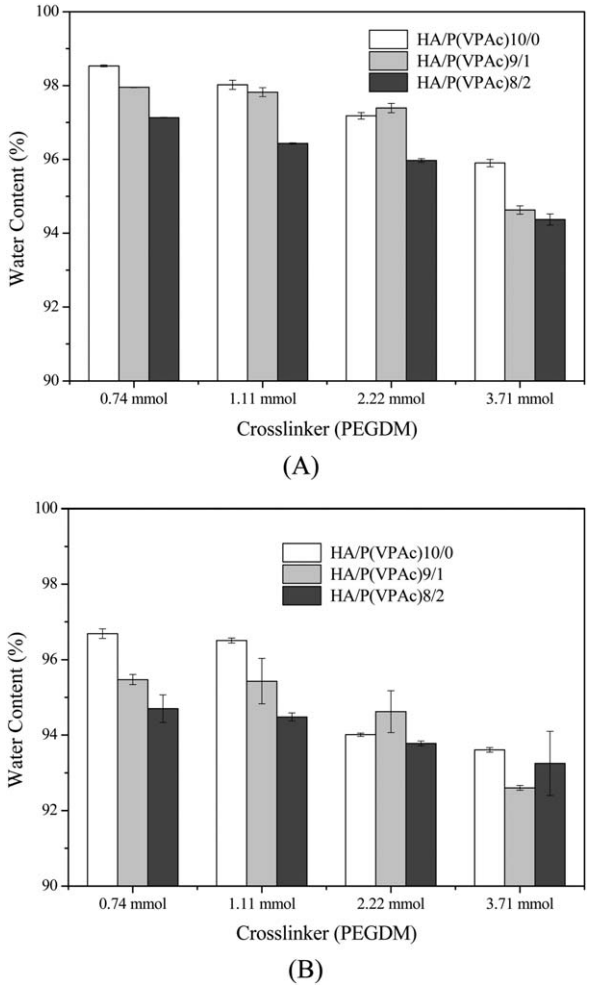

Figure 5. Water content of HA/P(VPAc) hydrogels with respect to the crosslinking density; (A) water content of HA/P(VPAc) hydrogels in ionized water and (B) water content of HA/P(VPAc) hydrogels in PBS.

depended on the crosslinking density of hydrogel. Figure 6(B) shows the degradation profiles of HA/P(PVAc)9/1 hydrogels prepared using different feed ratios of crosslinker PEGDM (as shown in Table I) in 150 U/ mL hyaluronidase solution. The degradation rate of HA/P(VPAc) hydrogel gradually decreased with increased crosslinking density. As the crosslinking density increases, additional degradable units must be broken to degrade the hydrogel. This results in a longer incubation time to achieve mass loss with increasing crosslinking density.

Drug Loading and Release from HA/P(VPAc) Hydrogels

Table II shows the drug loading content (DLC) of BSA in HA/P(VPAc) and biomineralized HA/P(VPAc) hydrogels with various composition. The DLC of HA/P(VPAc) hydrogels gradually increased as the HA content increased and the P(VPAc) content decreased [HA/P(VPAc)10/0-2 = 38.21 ± 1.78%; HA/P(VPAc)9/1-2 = 35.74 ± 0.57%; HA/ P(VPAc)8/2-2 = 30.77 ± 1.76%]. This trend for DLC of HA/P(VPAc) is consistent with the water content of the hydrogels, which also increased as the amount of HA (pK_a =3.0) containing ionizable groups (—COO^-) increased and the amount of P(VPAc) (pK_1 = 3.1 and pK_2 = 9.0) content, which did not fully ionize in deionized water (pH = 5.8), decreased. This indicates that repulsion between ionized —COO^- groups within the HA/P(VPAc) results in an increase in free volume in the polymeric matrix and a corresponding increase in the BSA loading content of the hydrogel.

The BSA loading content of the biomineralized HA/P(VPAc) hydrogelswas lower than that of untreated HA/P(VPAc) hydrogels (Table II) [B-HA/P(VPAc)10/0-2 = 17.46 ± 0.41%; B-HA/P(VPAc)9/1-2 = 16.32 ± 2.87%; B-HA/ P(VPAc)8/2-2 = 16.08 ± 1.56%]. This might reflect the decrease in water content of the hydrogels after biomineralization. In addition, unlike the untreated HA/P(VPAc) hydrogels, the composition of biomineralized HA/P(VPAc) hydrogel did not significantly influence the BSA loading content. This suggests that the nucleation and growth of calcium phosphate in hydrogels during biomineralization inhibits interaction between free ionized groups and BSA, leading to a decrease in the effect of ionic groups on the DLC.

The *in vitro* release kinetics of the model protein BSA from HA/P(VPAc) and biomineralized HA/P(VPAc) hydrogels over 14 days

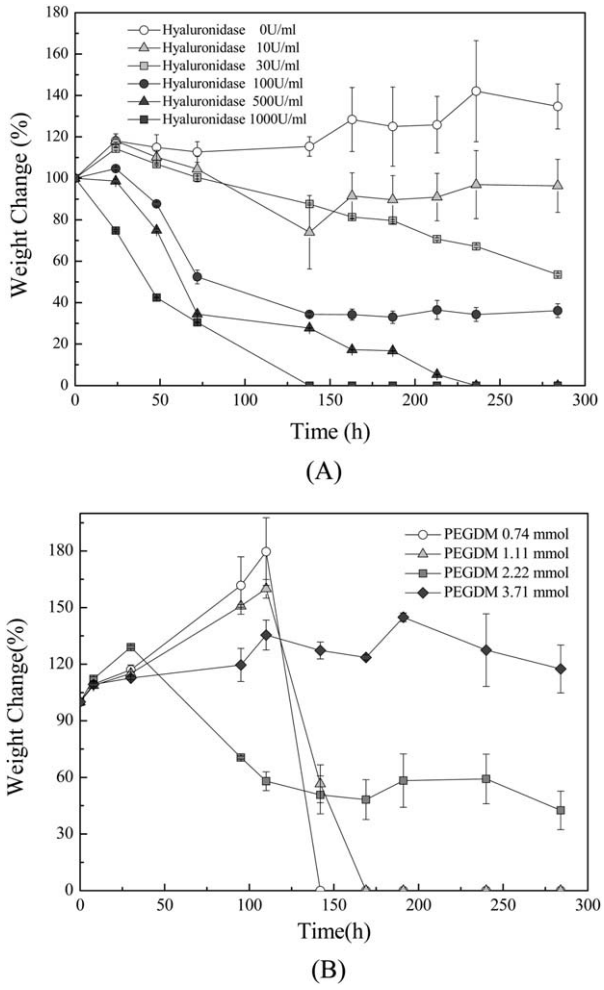

Figure 6. Enzymatic degradation of HA/P(VPAc) hydrogels; (A) degradation behavior of HA/P(VPAc)8/2-2 hydrogel with respect to the concentration of hyaluronidase solution and (B) degradation behavior of HA/P(VPAc)9/1-2 hydrogel with respect to the crosslinking density of hydrogels in 100 U/mL hyaluronidase solution. Each point represents the mean ± S.D. of three samples.

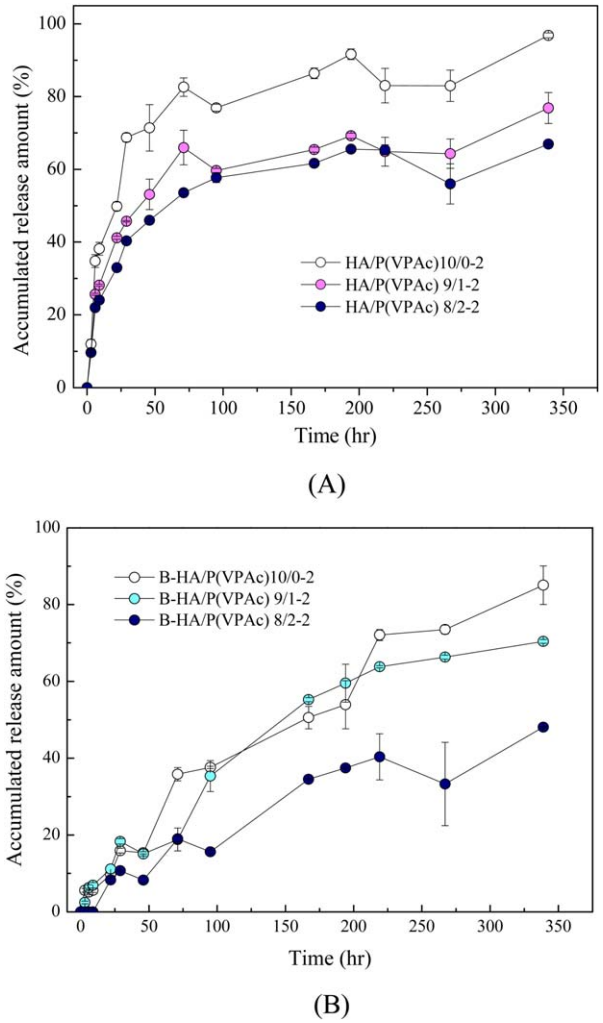

Figure 7. *In vitro* release kinetics of BSA from hydrogels at 37°C; (A) release behavior of BSA from HA/P(VPAc), (B) release behavior of BSA from biomineralized HA/P(VPAc) hydrogels. Each point represents the mean ± S.D. of three samples. [Color figure can be viewed in the online issue, which is available at wileyonlinelibrary.com.]

were investigated. HA/P(PVAc) and biomineralized HA/P(VPAc) hydrogels with crosslinked network structure remained as a coherent mass and could be physically manipulated during the release study. The release profiles of BSA from HA/P(VPAc) hydrogels with various compositions showed sustained release behavior and were influenced by the composition of the hydrogels [Figure 7(A)].

The release rate of BSA from HA/P(VPAc) hydrogels gradually increased [HA/P(VPAc)8/2-2 < HA/P(VPAc)9/1-2 < HA/P(VPAc)10/0–2] as the water content and DLC of hydrogels increased [HA/P(VPAc)8/2-2 = 96.43 ± 0.02 (%) water content, 30.77 ± 1.76(%) DLC; HA/P(VPAc)9/1-2 = 97.82 ± 0.11 (%) water content, 35.74 ± 0.57 (%) DLC; HA/P(VPAc)10/0-1 = 98.02 ± 0.12 (%) water content, 38.21 ± 1.78 (%) DLC]. This might be caused by an increase in the driving forces for diffusion of drug molecules, such as the concentration difference and swelling of the hydrogels.[37]

As shown in Figure 7(B), the release behaviors of BSA from the biomineralized HA/P(VPAc) hydrogels exhibited a similar trend to those of HA/P(VPAc) hydrogels. The release behavior of BSA gradually increased as the water content and DLC of hydrogels increased [B-HA/P(VPAc)8/2-2 < B-HA/P(VPAc)9/1-2 < B-HA/P(VPAc)10/0-2]. In addition, as expected, the release rate of BSA from the B-HA/P(VPAc) hydrogels with relatively low water content and DLC was much slower than that of the non-biomineralized hydrogels. This indicates that the release behavior of protein drug molecules from the HA/P(VPAc) hydrogel can be controlled by the composition, loading content, and biomineralization of hydrogel.

Cytotoxicity of HA/P(VPAc) Hydrogels

The biocompatibility of the HA/P(VPAc) and biomineralized HA/P(VPAc) hydrogels was evaluated by an indirect extraction method. HepG2 cells were incubated in medium containing hydrogel extract and *in vitro* cytotoxicity was investigated using a MTT assay, which measures the mitochondrial activity of vital cells and thus represents their metabolic activity.[18] Figure 8 shows the viability of HepG2 cells cultured with extracts of HA/P(VPAc) and biomineralized HA/P(VPAc) hydrogels. Incubation

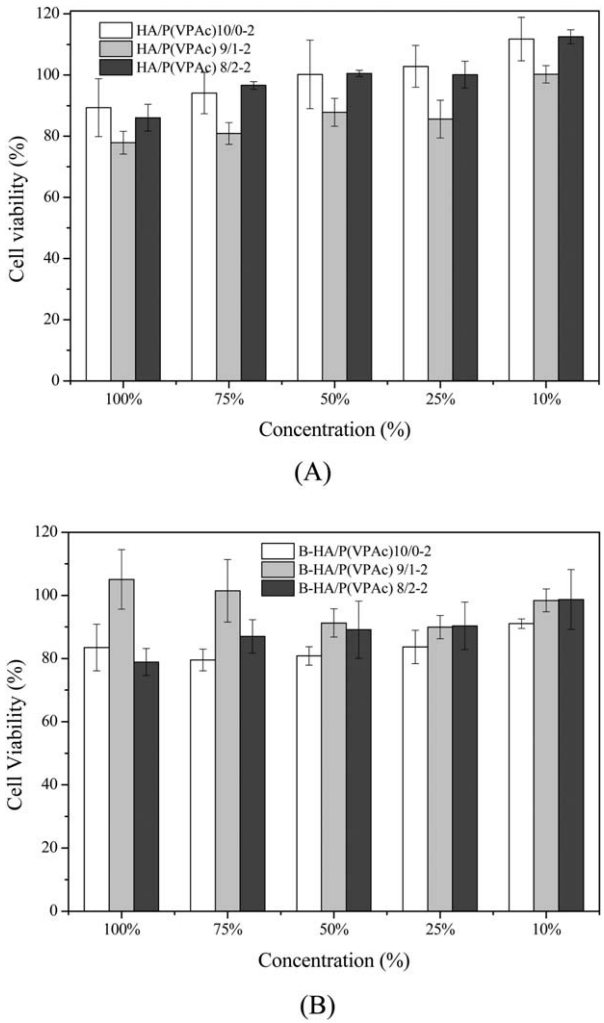

Figure 8. Viability of HepG2 cells cultured with extracts of hydrogels at different concentrations; (A) viability of HepG2 cells cultured with extracts of HA/P(VPAc) hydrogels and (B) viability of HepG2 cells cultured with extracts of biomineralized HA/P(VPAc) hydrogels. Values represent mean and standard deviation ($n = 4$).

with all HA/P(VPAc) and biomineralized HA/P(VPAc) hydrogel extracts tested resulted in relatively high cell viability (greater than 77%) within the 48 h observation period. Moreover, cell viability was not significantly influenced by the concentration of hydrogel extracts, as shown in Figure 8. This suggested that the HA/P(VPAc) and biomineralized HA/P(VPAc) hydrogels did not have any significant adverse effects on cell viability.

CONCLUSIONS

We prepared biomineralized HA/P(VPAc) hydrogels with the aim of developing a biomimetic hydrogel system for local drug delivery to improve bone regeneration. First, crosslinked hydrogels composed of the natural polymer HA and P(VPAc), which serves as a binding site for calcium ions during the mineralization procedure, were synthesized. Next, organic/inorganic hybrid HA/P(VPAc) hydrogels were prepared through a biomineralization process to mimic bone extracellular matrix. HA/P(VPAc) hydrogels exhibited a relatively high water content of >90% and the water content was influenced by the HA/P(VPAc) composition, crosslinking density, biomineralization, and ionic strength of the swelling media. Although the water content of biomineralized HA/P(VPAc) hydrogels was decreased by the nucleation and growth of calcium phosphate in the hydrogels, biomineralied HA/P(VPAc) hydrogels still maintained a water content greater than 84%. The enzymatic degradation behavior of HA/P(VPAc) hydrogels depended on the concentration of hyaluronidase and the crosslinking density of the hydrogel. The release kinetics of a model protein drug, BSA, from the HA/P(VPAc) hydrogels was primarily dependent on the DLC, water content, and biomineralization of the hydrogels. Cytotoxicity tests showed that HA/P(VPAc) and biomineralized HA/P(VPAc) hydrogels did not have significant adverse effects on the viability of HepG2 cells. Therefore, biomineralized HA/P(VPAc) hydrogels may be applied to a biomimetic ECM to improve bone repair and bone regeneration through local delivery of a protein drug including bone morphogenetic proteins.

ACKNOWLEDGMENTS

This research was supported by Basic Science Research Program through the National Research Foundation of Korea (NRF) funded by the Ministry of Science, ICT, and Future Planning (NRF-2012R1A1A3013658).

REFERENCES

1. Holzwarth, J. M.; Ma, P. X. *Biomaterials* **2011**, *32*, 9622.
2. Bose, S.; Roy, M.; Bandyopadhyay, A. *Trends Biotechnol.* **2012**, *30*, 546.
3. Liu, Y.; Lim, J.; Teoh, S. H. *Biotechnol. Adv.* **2013**, *31*, 688.
4. Hutmacher, D. W. *Biomaterials* **2000**, *21*, 2529.
5. Wang, H.; Li, Y.; Zuo, Y.; Li, J.; Ma, S.; Cheng, L. *Biomaterials* **2007**, *28*, 3338.
6. Tessmar, J. K.; Gopferich, A. M. *Adv. Drug Delivery Rev.* **2007**, *59*, 274.
7. Mehta, M.; Schmidt-Bleek, K.; Duda, G. N.; Mooney, D. J. *Adv. Drug Delivery Rev.* **2012**, *64*, 1257.
8. Kofron, M. D.; Laurencin, C. T. *Adv. Drug Delivery Rev.* **2006**, *58*, 555.
9. Niu, X.; Feng, Q.; Wang, M.; Guo, X.; Zheng, Q. *J. Controlled Release* **2009**, *134*, 111.
10. Malafaya, P. B.; Silva, G. A.; Baran, E. T.; Reis, R. L. *Curr. Opin. Solid Mater. Sci.* **2002**, *6*, 283.
11. Lin, Y. H.; Liang, H. F.; Chung, C. K.; Chen, M. C.; Sung, H. W. *Biomaterials* **2005**, *26*, 2105.
12. Dorkoosh, F. A.; Verhoef, J. C.; Ambagts, M. H. C.; Rafiee-Tehrani, M.; Borchard, G.; Junginger, H. E. *Eur. J. Pharm. Sci.* **2002**, *15*, 433.
13. Maire, M.; Chaubet, F.; Mary, P.; Blanchat, C.; Meunier, A.; Logeart-Avramoglou, D. *Biomaterials* **2005**, *26*, 5085.
14. Gumusderelioglu, M.; Kesgin, D. *Int. J. Pharm.* **2005**, *288*, 273.
15. Drury, J. L.; Mooney, D. J. *Biomaterials* **2003**, *24*, 4337.
16. Song, J.; Saiz, E.; Bertozzi, C. R. *J. Eur. Ceram. Soc.* **2003**, *23*, 2905.
17. Dogan, O.; Oner, M. *Langmuir* **2006**, *22*, 9671.
18. Nuttelman, C. R.; Benoit, D. S. W.; Tripodi, M. C.; Anseth, K. S. *Biomaterials* **2006**, *27*, 1377.
19. Yokoi, T.; Kawashita, M.; Kikuta, K.; Ohtsuki, C. *Mater. Sci. Eng. C* **2010**, *30*, 154.
20. Ma, Y.; Feng, Q. *J. Solid State Chem.* **2011**, *184*, 1008.
21. Furuzono, T.; Taguchi, T.; Kishida, A.; Akashi, M.; Tamada, Y. *J. Biomed. Mater. Res.* **2000**, *50*, 344.
22. Taguchi, T.; Muraoka, Y.; Matsuyama, H.; Kishida, A.; Akashi, M. *Biomaterials* **2001**, *22*, 53.
23. Abdelkebir, K.; Morin-Grognet, S.; Gaudiere, F.; Coquerel, G.; Labat, B.; Atmani, H. *Acta Biomater.* **2012**, *8*, 3419.
24. Bleek, K.; Taubert, A. *Acta Biomater.* **2013**, *9*, 6283.
25. Sasaki, S.; Yataki, K.; Maeda, H. *Langmuir* **1998**, *14*, 796.
26. Phadke, A.; Zhang, C.; Hwang, Y.; Vecchio, K.; Varghese, S. *Biomacromolecules* **2010**, *11*, 2060.
27. Collins, M. N.; Birkinshaw, C. *Carbohydr. Polym.* **2013**, *92*, 1262.
28. Price, R. D.; Berry, M. G.; Navsaria, H. A. *J. Plast. Reconstr. Aesthet. Surg.* **2007**, *60*, 1110.
29. Leach, J. B.; Schmidt, C. E. *Biomaterials* **2005**, *26*, 125.
30. Kim, S. Y.; Healy, K. E. *Biomacromolecules* **2003**, *4*, 1214.
31. Kim, S. Y.; Chung, E. H.; Gilbert, M.; Healy, K. E. *J. Biomed. Mater. Res.* **2005**, *75A*, 73.
32. Pariente, J.-L.; Kim, B.-S.; Atala, A. *J. Biomed. Mater. Res.* **2001**, *55*, 33.
33. Zange, R.; Li, Y.; Kissel, T. *J. Controlled Release* **1998**, *56*, 249.
34. Graillot, A.; Bouyer, D.; Monge, S.; Robin, J.; Faur, C. *J. Hazard. Mater.* **2013**, *244–245*, 507.
35. Chaterji, S.; Kwon, I. K.; Park, K. *Prog. Polym. Sci.* **2007**, *32*, 1083.
36. Rasool, N.; Yasin, T.; Heng, J. Y. Y.; Akhter, Z. *Polymer* **2010**, *51*, 1687.
37. Lin, C.-C.; Metters, A. T. *Adv. Drug Delivery Rev.* **2006**, *58*, 1379.